Chem Biol Drug Des 2011; **78:** 57–72

Research Article

doi: 10.1111/j.1747-0285.2011.01089.x

New Uses for Old Drugs: Pharmacophore-Based Screening for the Discovery of P-Glycoprotein Inhibitors

Andreia Palmeira[1,2,3], Freddy Rodrigues[4], Emília Sousa[1,2], Madalena Pinto[1,2], M. Helena Vasconcelos[3,5] and Miguel X. Fernandes[4,*]

[1]*Laboratório de Química Orgânica e Farmacêutica, Departamento de Química, Faculdade de Farmácia, Universidade do Porto, Rua Aníbal Cunha 164, 4050-047 Porto, Portugal*
[2]*Centro de Química Medicinal - Universidade do Porto (CEQUIMED-UP), Rua Anibal Cunha 164, 4050-047 Porto, Portugal*
[3]*IPATIMUP – Institute of Molecular Pathology and Immunology of the University of Porto, Rua Dr Roberto Frias s/n, 4200-465 Porto, Portugal*
[4]*Centro de Química da Madeira, Universidade da Madeira, Campus da Penteada, 9000-390 Funchal, Portugal*
[5]*Laboratório de Microbiologia, Departamento de Ciências Biológicas, Faculdade de Farmácia, Universidade do Porto, Rua Anibal Cunha 164, 4050-047 Porto, Portugal*
**Corresponding author: Miguel X. Fernandes, mxf@uma.pt*

P-glycoprotein (P-gp) is one of the best characterized transporters responsible for the multidrug resistance phenotype exhibited by cancer cells. Therefore, there is widespread interest in elucidating whether existing drugs are candidate P-gp substrates or inhibitors. With this aim, a pharmacophore model was created based on known P-gp inhibitors and it was used to screen a database of existing drugs. The P-gp modulatory activity of the best hits was evaluated by several methods such as the rhodamine-123 accumulation assay using K562Dox cell line, and a P-gp ATPase activity assay. The ability of these compounds to enhance the cytotoxicity of doxorubicin was assessed with the sulphorhodamine-B assay. Of the 21 hit compounds selected *in silico*, 12 were found to significantly increase the intracellular accumulation of Rhodamine-123, a P-gp substrate. In addition, amoxapine and loxapine, two tetracyclic antidepressant drugs, were discovered to be potent non-competitive inhibitors of P-gp, causing a 3.5-fold decrease in the doxorubicin GI_{50} in K562Dox cell line. The overall results provide important clues for the non-label use of known drugs as inhibitors of P-gp. Potent inhibitors with a dibenzoxazepine scaffold emerged from this study and they will be further investigated in order to develop new P-gp inhibitors.

Key words: cancer, multidrug-resistance transporters, oxazepine, P-glycoprotein inhibitors, pharmacophore, virtual screening

Received 15 July 2010, revised 22 November 2010 and accepted for publication 5 January 2011

Resistance to chemotherapy represents a major obstacle to the treatment of cancer. Multidrug resistance (MDR) can be broadly defined as a phenomenon by which tumor cells *in vivo* and cultured cells *in vitro* show simultaneous resistance to a variety of structurally and functionally dissimilar cytotoxic and xenobiotic compounds (1). It has been estimated that at least 50% of human cancers express the MDR phenotype (2,3). MDR can be present at the time of diagnosis, or can be acquired after initial treatment and remission of cancer (4). P-glycoprotein (P-gp), a 170-kDa membrane protein, represents one of the best characterized barriers to chemotherapeutic treatment in cancer (5). P-gp is coded by the *mdr1* gene and functions as an energy-dependent membrane transporter that actively extrudes a set of structurally unrelated compounds out of the cells, conferring the MDR phenotype in cancer (6). P-gp integrates the ATP-binding cassette (ABC) super family of transporters; other members of this super family are also implied in some cases of resistance, as happens with the multidrug-resistance protein 1 (MRP-1) (7). The molecular structure of P-gp consists of 12 transmembrane domains that form a drug-binding pore and the translocation pathway, and two cytoplasmic ATP-binding domains (8). Physiologically, it is believed that P-gp may play a significant role in the processes of drug absorption, distribution, metabolism, and excretion (ADME) (9–11). P-gp physiologic localization suggests that this efflux transporter can protect the body against toxic xenobiotics by excreting these compounds into the bile, urine, and the intestinal lumen, and by preventing their accumulation in brain. On the other hand, in humans, CYP3A4 is the principal enzyme involved in the hepatic and intestinal metabolism of drugs (12). Furthermore, P-gp and CYP3A4 are frequently co-expressed in the same cells and share a large number of substrates and modulators (13,14). The disposal of such drugs is thus severely affected in those cells. Consequently, the inhibition of P-gp could have implications related to ADME (9). If a drug is a P-gp substrate or if it interferes with the P-gp efflux phenomenon, it may affect the efficacy of the drug, as well as its concentration in the bloodstream, and clearance mechanisms (15,16). Additionally, side-effects are a complex phenomenon that occur in a variety of molecular scenarios, the most important of which being the direct interaction with other protein targets such as, for instance, P-gp (17,18). Therefore, screening for P-gp modula-

tors has become an essential goal of drug discovery (19,20). On top of that, interaction with P-gp is worth studying, even for commercially available drugs, as it may help explain some *in vivo* events such as drug bioavailability or drug–drug interactions.

Despite its overall significance, P-gp is poorly characterized at the atomic level, especially because of the intrinsic difficulties involved in membrane protein crystallization (21,22). P-gp structural data are only available at low-to-medium resolution. Hence, there is a need for ligand-based design, namely pharmacophore construction as previously performed by other groups (23–26).

For all these reasons, the objective of the present work was the implementation of a method for quick identification of P-gp modulators. A virtual screening using a pharmacophore model was performed, and the P-gp modulatory effects of the retrieved 21 hit drugs were experimentally explored using several techniques such as a rhodamine-123 (rh123) accumulation assay using a leukemia P-gp overexpressing cell line (K562Dox), a P-gp ATPase assay using P-gp membranes, and the sulphorhodamine-B (SRB) cell growth assay studying the potential P-gp modulators in combination with doxorubicin in K562Dox cells.

Material

Cell lines

K562 (human chronic myelogenous leukemia, erythroblastic; ECACC, Europe Collection of Cell Cultures, UK), and K562Dox (derived from K562 by doxorubicin stimulated overexpression of P-gp; kind gift from Prof. J. P. Marie, Paris, France) cell lines were routinely maintained in RPMI-1640 (with Hepes and Glutamax, Gibco®; Invitrogen, Darmstadt, Germany), with 10% or 5% fetal bovine serum (Gibco®; Invitrogen, Darmstadt, Germany) and incubated in a humidified incubator at 37 °C with 5% CO_2 in air. All experiments were performed with cells in exponential growth, with viabilities over 90% and repeated at least three times. K562-Dox cells were maintained by treating them with 1.0 μM doxorubicin every 2 weeks in order to maintain the P-gp overexpression, and all experiments were performed at least 4 days after this administration and in doxorubicin-free medium.

Compounds

Amoxapine, azelastine, bicalutamide, blebbistatine, coelemerazide, cyclic pifithryn-α, danthron, diltiazem, econazole, hycanthone, indapamide, indirubin, leflutamide, loxapine, pranlukast, prazosin, propafenone, quinidine, sulfinpyrazone, tioconazol, verapamil, warfarin and zomepirac, as well as SRB and rhodamine-123 (rh123) were obtained from Sigma-Aldrich (Sintra, Portugal). Verapamil, quinidine, and mibefradil (known P-gp inhibitors) were used as controls.

Methods

Pharmacophore modeling and virtual screening of a database of compounds

A pharmacophore is the 3D arrangement with the minimal molecular features needed for a compound to show biologic activity. This 3D arrangement of features has a set of distance restraints between them, meaning that these features must be separated by specific distances in order to have a molecule with putative activity. To create the pharmacophore, model we started with 26 P-gp known inhibitors from the flavonoid family (27,28) (Appendix S1). The structures of these compounds were drawn using HyperChem 7.51 (29) and pre-optimized using Molecular Mechanics force field (MM+). Afterward, the molecular geometries were refined using AM1 semi-empirical (Polak-Ribiere – Conjugate Gradient) calculations (30). The structures were considered optimized when their conformational energy gradient was below 0.01 kcal/Å. We uploaded the structural data of these 26 known inhibitors of P-gp into the Pharmagist webserver PharmaGist to obtain the pharmacophore model. (31). In PharmaGist, the pharmacophore is constructed using six different features (H-bond acceptor, H-bond donors, aromatic centers, hydrophobic centers, negative charge, and positive charge). The pharmacophore from PharmaGist was used to screen the DrugBank database (32). The database files were edited using small scripts to remove counter-ions, neutralize partial charges and remove solvent molecules. Additionally, all structures were converted to 3D using the software Corina (Molecular Networks GmbH, Erlangen, Germany). After preparing the database, the program VLifeMDS (VLife Ltd., Pune, India) was used to virtually screen the database using the pharmacophore model generated previously with a distance tolerance between features of 20%.

Protein expression analysis by Western blot

For analysis of protein expression, K562 and K562Dox cells were lysed in Winman's buffer (1% NP-40, 0.1 M Tris–HCl pH 8.0, 0.15 M NaCl and 5 mM EDTA) with EDTA-free protease inhibitor cocktail (Boehringer, Mannheim, Germany). Proteins were quantified using the DC Protein Assay kit (BioRad, Hercules, CA, USA) and separated in 8% Tris-glycine SDS-polyacrylamide gels. The A549 cell lysate was used as positive control for detection of MRP-1. Proteins were then transferred to a nitro-cellulose membrane (GE Healthcare, Piscataway, NJ, USA). The membranes were incubated with the following primary antibodies for MDR-1 (1:5000; Santa Cruz Biotechnology Inc., Heidelberg, Germany), MRP-1 (1:500; Santa Cruz Biotechnology Inc., Heidelberg, Germany) and Actin (1:2000; Santa Cruz Biotechnology Inc., Heidelberg, Germany). Membranes were further incubated with the respective secondary antibodies-HRP conjugated (1:2000; Santa Cruz Biotechnology, Heidelberg, Germany). The signal was detected with the Amersham ECL kit (GE Healthcare, Piscataway, NJ, USA), Hyperfilm ECL (GE Healthcare, Piscataway, NJ, USA) and Kodak GBX developer and fixer twin pack (Sigma-Aldrich, Sintra, Portugal) as previously described (33). The intensity of the bands obtained in each film was further analyzed using the software Quantity One – 1D Analysis (BioRad, Hercules, CA, USA).

Flow cytometry determination of rhodamine-123 accumulation

K562 and K562Dox (5×10^6 cells/mL) were incubated for 1 h at 37 °C in the presence of 10 or 20 μM of the test compounds, and with 1 μM rhodamine-123 (rh123). K562Dox and K562 cells alone, as well as K562Dox cells in the presence of the known P-gp inhibitors verapamil, mibefradil, or quinidine (10 and 20 μM), were used as

controls. After the incubation time, cells were washed twice, re-suspended in ice-cold PBS and kept at 4 °C in the dark until analysis in the flow cytometer. At least 20 000 cells per sample were counted and analyzed by flow cytometry (Epics XL-MCL; Beckman Coulter, Brea, CA, USA). Cells shown in forward scatter and side scatter were electronically gated and acquired through the FL1 channel. The amount of fluorescence was plotted as a histogram of FL1 within the gate. Data acquisition was performed using WINMDI 2.9 (TSRI, Jupiter, FL, USA) to determine median fluorescence intensity values (MFI). For simple interpretation, the ratio of accumulation was calculated as $(MFI_{K562Dox\ +\ Drug} - MFI_{K562Dox})/MFI_{K562Dox}$. Results represent the average of at least three independent experiments.

Determination of ATPase activity

The ATPase activity of P-gp was determined using the luminescent ATP detection kit (P-gp-Glo Assay Kit, Promega, Germany) according to the manufacturers' recommendation[a]. Test compounds at 200 μM or sodium vanadate (Na_3VO_4) at 20 μM (positive control, non-competitive inhibitor) or verapamil at 200 μM (negative control, competitive inhibitor) in buffer solution were incubated with 0.5 mg/mL P-gp and 5 mM MgATP at 37 °C for exactly 40 min, and the remaining ATP was detected after 20 min resting at room temperature, as a luciferase-generated luminescent signal. Results are presented as the average of three independent experiments. Percentage of relative light unit (RLU) was calculated in relation to non-treated control (NT). It was calculated using the following formula that fits the NT control to zero for easier interpretation: $\%\ RLU = (RLU_{test} - RLU_{NT})/RLU_{NT} \times 100$.

Cell growth assay

The ability of the tested compounds to potentiate doxorubicin cytotoxicity was evaluated in K562Dox cells SRB assay as previously described (34). K562Dox cells were plated into 96-well tissue culture plates at 5×10^4 cells/mL. After 24 h, cells were treated with serial dilutions of the test compound alone or with serial dilutions of doxorubicin, a known chemotherapeutic agent, in combination with 10 μM of the test compound. Following 48-h treatment, cell growth was assayed using the SRB assay. The GI_{50} values for doxorubicin (concentration resulting in 50% inhibition of cell growth) were calculated from the plotted results. The reversal fold (RF) values, as potency of reversal, were obtained by calculating the coefficient $RF = GI_{50}$ of doxorubicin alone/GI_{50} of doxorubicin in the presence of a test compound.

Principal component analysis

Principal component analysis (PCA) is a common statistical technique for finding patterns in data of high dimension, where graphical representation is not available, and representing the data in such a way as to highlight their similarities and differences. The main advantage of PCA is the reduction of the number of dimensions (observed variables, or in our case molecular descriptors) without significant loss of information. A principal component (artificial variable) can be defined as a linear combination of optimally weighted observed variables. Principal component analysis was performed on both inhibitors and activators of P-gp using the Accelrys Library Analysis Module (Accelrys, San Diego, CA, USA). Following the parsimony principle, six molecular descriptors available as default in Accelrys library analysis by PCA, and commonly used in drug-like profiling (atom-based module for logP (ALogP), molecular weight, number of hydrogen bond donors (HBD), number of hydrogen bond acceptors (HBA), number of rotatable bonds and molecular polar surface area), were used to assess the chemical diversity of the 24 compounds screened. In a PCA calculation, principal components are always orthogonal between them (therefore without cross-correlation), and the first three principal components were chosen because they show the highest gradients of variance for the data (they account for the maximum variability in the dependent variable, meaning biologic response). Finally, a 3D graphical projection was analyzed.

Statistical analysis

Data were expressed as the mean ± SE and analyzed by the Student's *t*-test. p-values below 0.05 considered statistically significant.

Results and discussion

Identifying molecules that interact with P-gp is important for drug discovery but is also generally reliant on time-consuming *in vitro* and *in vivo* studies. As an alternative approach, the current study applies a pharmacophore model and *in silico* database screening to rapidly retrieve molecules from commercial databases that potentially bind (as substrates or inhibitors) to P-gp. The advantage of such an approach lies on the discovery of a new drug having an 'old drug' as a hit (35). In fact, any newly identified non-label use for an 'old drug' can be rapidly evaluated with a dramatic decrease in time and costs by eliminating much of the toxicological and pharmacokinetic assessments (35). Once the results from a screening show a new hit, it can be used as the starting point for a drug discovery program, turning the 'side activity' into the 'main activity' and, ideally, the initial 'main activity' will be significantly reduced or abolished. This is the so-called selective optimization of side activities (the SOSA approach) of drug molecules and constitutes an intelligent and efficient strategy for the generation of new therapeutic applications (36). This strategy has a high probability of yielding safe, bioavailable, original and patentable analogues (37). The scheme of the *in silico* and laboratorial procedures is summarized in Figure 1.

Pharmacophore modeling and virtual screening of a database of compounds

After performing a pairwise and multiple flexible alignments with 26 P-gp's known inhibitors from the flavonoid family, using the PharmaGist webserver, a pharmacophore model was found (Figures 1I and 2A). There were three common features present in all 26 inhibitors, two aromatic rings (AR) and one H-bond acceptor (HBA). The 3D pharmacophore and the distance constraints between the features are represented in Figure 2B.

After the procedures described to clean the database, 4825 structures of small molecules (no peptides or proteins) from DrugBank were screened to determine their compliance with the pharmacophore model. Of the hits retrieved, 167 structures were found to comply with the pharmacophore model with a RMSD of <1 Å. Of

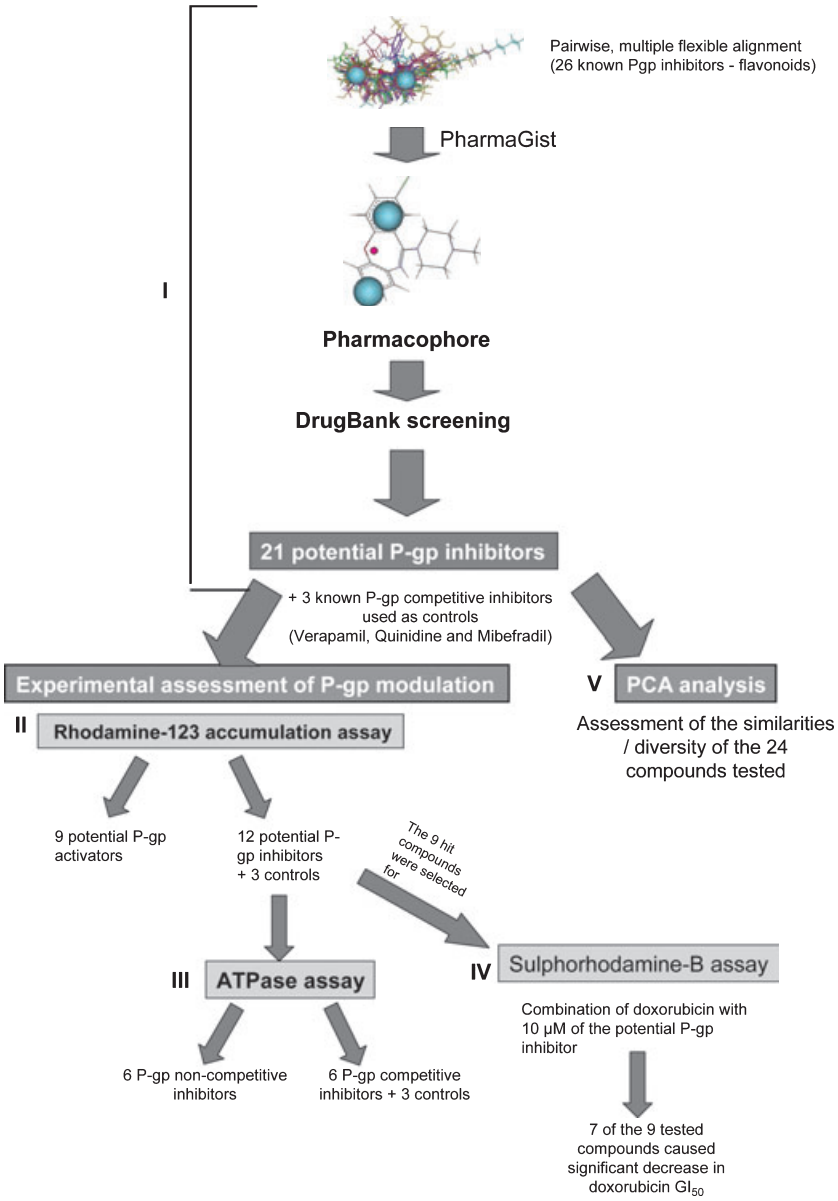

Figure 1: Scheme of the *in silico* and laboratorial procedures. (I) Pharmacophore-based virtual screening. (II) Rhodamine-123 accumulation assay. (III) P-gp ATPase assay. (IV) Sulphorhodamine-B assay. (V) Principal component analysis.

these 167 structures, 91 fulfilled the Lipinski rules (38). The hits that did not comply with the Lipinski rules were discarded.

Twenty-one commercially available drugs were selected (Table 1) for further *in vitro* testing according to their RMSD (the lower the better) and availability for purchase. Half of them had already been described as being implied in reversal of MDR as indicated in Table 1.

Verapamil, a calcium channel blocker (anti-arrhythmic agent), and quinidine, a muscarinic and α-adrenergic neurotransmission blocker, belong to the first generation of known P-gp inhibitors (53) and were used in this study as controls. Mibefradil, a calcium T- and L-channel blocker developed for use in hypertension was also used as control because it is a potent inhibitor of P-gp-mediated digoxin transport (54).

According to the literature, there is no explicit information on how leflunomide, blebbistatine, diltiazem, tioconazole, pranlukast, coelenteramide, econazole, loxapine, amoxapine, indapamide, sulfinpirazone, indirubin, bicalutamide, and danthron interact with P-gp. The fact that some of the drugs here found by pharmacophore screening had previously been described as having some relation to P-gp or other ABC transporters makes the described pharmacophore model more reliable. They were therefore included in this study to confirm the results.

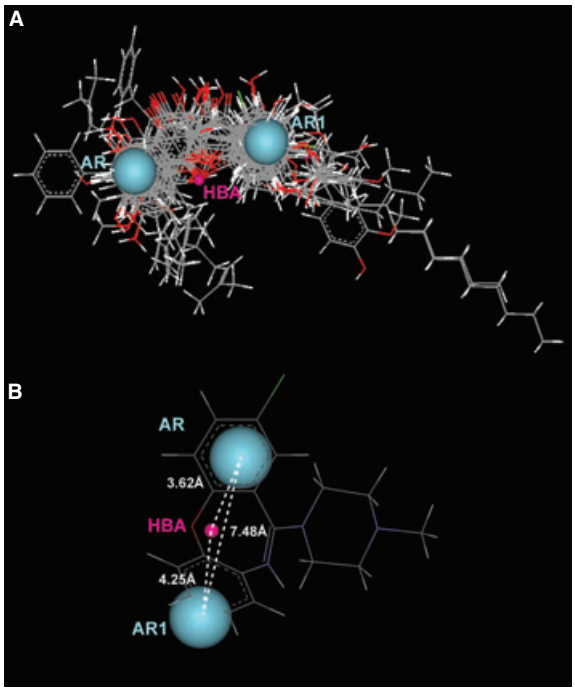

Figure 2: Pharmacophore-based virtual screening. (A) Superimposion of flavonoids used to build a pharmacophore. (B) Pharmacophore model for P-gp inhibitors obtained with PharmaGist, aligned with one of the compounds found on the Drug Bank virtual screening (oxapine). AR: aromatic ring; HBA: hydrogen bond acceptor.

Flow cytometry determination of rhodamine-123 accumulation on P-gp overexpressing cell line

An indirect way to analyze P-gp activity is by the evaluation of the mean fluorescence intensity (MFI) of cells exposed to rh123, a known P-gp substrate, together with the potential P-gp inhibitor (Figure 1II, 55–57). Quantification of the relative fluorescence can be used to compare the individual potency of inhibitors. This flow cytometry method for P-gp functional evaluation has been used for decades (58,59) and was chosen to initiate the present study. Rh123 is very efficiently transported by P-gp, resulting in a larger cellular accumulation of this probe compared to other probes such as doxorubicin or daunorubicin. Rh123 was therefore selected as a substrate for the determination of its accumulation in a human leukemia cell line (60). We used K562Dox cells (which overexpress P-gp) and the parental K562 cells to study the effects of drugs on P-gp function, by determining intracellular rh123-associated MFI. However, rh123 is a substrate not only for P-gp but also for MRP (61) and expression of both P-gp and MRP has been reported to occur in leukemic cells (62). So, transport of rh123 in such cells may be influenced by both MRP and P-gp. In order to confirm the presence of P-gp and to investigate the possible presence of MRP-1 in these cells, Western blot for both P-gp and MRP-1 was performed (Figure 3). P-gp appears as a diffuse band around 170 KDa and, as expected, it is present in K562Dox but not in K562 cell lines. As far as MRP-1 is concerned, a broad band between 150 and 250 kDa is observed in the positive control (A549 cell lysate), but no MRP-1 was observed in either K562 or K562Dox. As K562Dox cell line overexpresses P-gp but no MRP-1 (Figure 3), differences in the accumulation pattern of rh123 among the several treatments should be related to levels of P-gp but not to MRP-1.

The influence of the test compounds in the accumulation of rh123 is shown in Figure 4. After K562 cells were incubated with rh123, accumulation ratio increased after 1 h, as it was expected for a cell line which does not express P-gp; untreated K562Dox cells had a residual accumulation (accumulation depends on the level of intracellular uptake and extracellular efflux) of rh123, represented as 'zero' on Figure 4 (second column) for easier interpretation. After the same cells (K562Dox) were incubated in the presence of the test compounds, the accumulation ratios varied, according to the applied formula. In the case of twelve investigated compounds (Figure 4, columns on the right), an increase in the accumulation ratio of rh123 was observed, an effect compatible with P-gp inhibition, whereas for six compounds a statistically significant decrease in the accumulation ratio was verified, an effect compatible with P-gp activation (Figure 4, columns on the center).

According to the cytometry assay (Figure 4), known P-gp inhibitors such as verapamil, quinidine and mibefradil as well as twelve investigated compounds were found to potentiate the accumulation of P-gp's substrate rh123. Particularly, propafenone, azelastine, amoxapine and loxapine showed an effect similar to that elicited by the known P-gp inhibitor, quinidine. From these, amoxapine has never been previously described as inhibitor of P-gp, whereas loxapine has already been described as multidrug-resistant reversal agent (46). Loxapine showed a high accumulation ratio, apparently in a concentration-dependent manner. Amoxapine also showed high accumulation ratio but not in a concentration-dependent manner, at least for the interval of concentrations used.

As expected, propafenone and azelastine, previously shown to be modulators of drug resistance, presented the highest rh123 accumulation ratios. Other drugs, such as hycanthone, bicalutamide, econazole, diltiazem, prazosin, and tioconazole, showed a moderate effect in the rh123 accumulation ratio, with econazole being described for the first time as a P-gp inhibitor. In contrast, coelemerazine, leflunomide, blebbistatine, and indirubin showed an effect compatible with P-gp activation. This is an important issue, as the bioavailability of these drugs may be compromised and higher doses may be needed to reach an adequate therapeutic effect.

Determination of ATPase activity

Although the rh123 accumulation assay is simple and fast, allowing for the rapid screening of several compounds simultaneously, it is indirect, because it is a measure of rh123 accumulation and not a specific test for the P-gp function (Figure 1III). In order to determine how a compound interacts with P-gp, it is possible to carry out the measurement of its effect on the rate of P-gp ATP hydrolysis which will allow to discriminate between drugs that increase the ATP consumption by P-gp (i.e., competitive inhibitors or substrates) and drugs that reduce the use of ATP either by acting directly on ATP-binding site or indirectly by blocking an allosteric site relevant for P-gp activity (i.e., non-competitive inhibitors) (63,64). Therefore, to

Table 1: Compounds selected from pharmocophore screening and their relevant chemical parameters and biologic activities

Structure	Molecular weight	ALogP	Hydrogen bond donors	Hydrogen bond acceptors	Name/activity (http://pubchem .ncbi.nlm.nih.gov/)	Described ATP-binding cassette transporters modulation
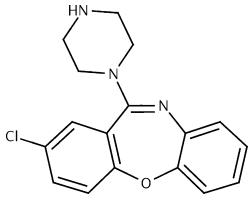	313.81	3.422	1	4	Amoxapine Antipsychotic agent Blocks the reuptake of norepinephrine and serotonin Also blocks dopamine receptors	No data
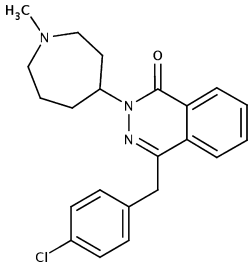	381.94	4.094	0	4	Azelastine Antihistamine Mast cell stabilizer Used on allergic conjunctivitis	Described as capable of reversing resistance to doxorubicin (39) although the mechanism is not known
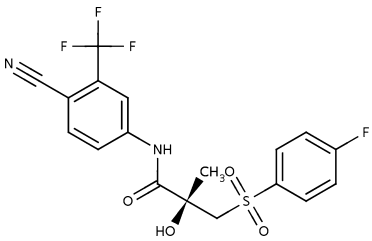	430.41	2.927	2	10	Bicalutamide Non-steroidal antiandrogen for prostate cancer	Failed in treatment because it is transported by both P-gp and BCRP. MRP1 is unable to bind to this antiandrogen drug (40)
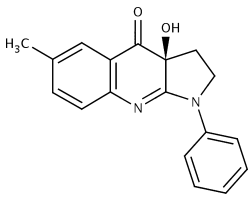	292.36	3.046	1	4	Blebbistatin Inhibitor of myosin II	No data
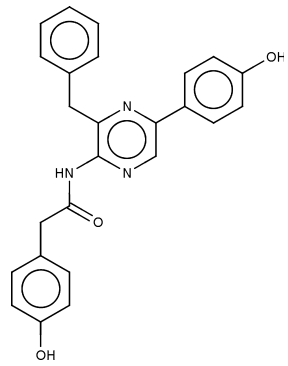	411.49	4.281	3	6	Coelenteramide A coelenterazine derivative, a light emitting molecule found in many aquatic organisms	No data

Table 1: (*Continued*)

Structure	Molecular weight	ALogP	Hydrogen bond donors	Hydrogen bond acceptors	Name/activity (http://pubchem.ncbi.nlm.nih.gov/)	Described ATP-binding cassette transporters modulation
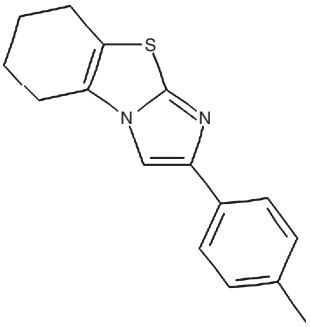	349.28	4.450	0	2	Cyclic pifithryn-α Inhibitor of p53 P-gp modulator Reported as a potent STAT6 transcriptional inhibitor	Described as modulator of P-gp-mediated efflux of daunorubicin and rh123 in a concentration-dependent manner by changing relative substrate specificity of the transporter (41)
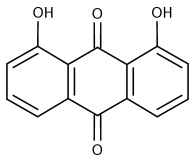	240.22	2.274	2	4	Danthron Laxative Withdrawn from the market because of genotoxicity	No data
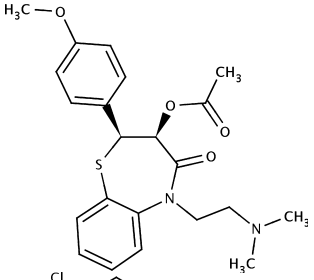	414.57	3.200	0	6	Diltiazem Vasodilating agent Antagonist of the actions of the calcium ion in membrane functions	Desacetyl-Diltiazem, a Diltiazem metabolite, seemed to be subjected to P-gp-mediated efflux (42)
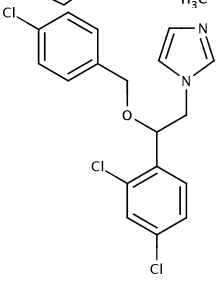	381.70	4.981	0	2	Econazole Antifungal agent Low activity against Gram positive bacteria	Itraconazole and Ketoconazole inhibit P-gp function (43); there is no reference to Econazole
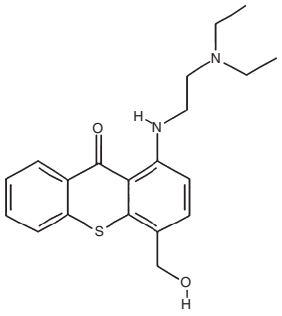	356.48	4.654	2	4	Hycanthone Antischistosomal agent	Blocks P-gp function, partially circumventing resistance of doxorubicin-resistant sarcoma 180 (S180) cells (44)

Table 1: (*Continued*)

Structure	Molecular weight	ALogP	Hydrogen bond donors	Hydrogen bond acceptors	Name/activity (http://pubchem.ncbi.nlm.nih.gov/)	Described ATP-binding cassette transporters modulation
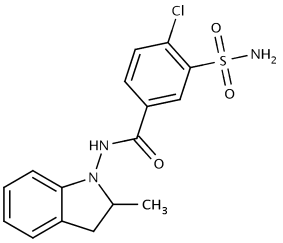	365.87	2.771	3	6	Indapamide Diuretic agent	No data
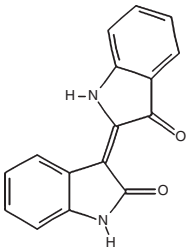	262.26	1.964	2	4	Indirubin Used in treatment of chronic granulocytic leukemia	No data
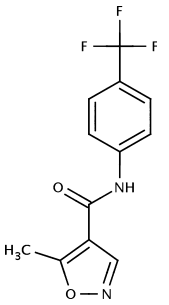	270.23	2.157	1	7	Leflunomide Pyrimidine synthesis inhibitor Disease-modifying antirheumatic drug	Described as high affinity substrate of BCRP (45). There is no reference to effects on P-gp
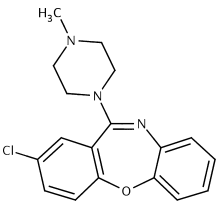	327.84	3.958	0	4	Loxapine Antipsychotic agent Used in schizophrenia	Reverses multidrug resistance on multidrug resistance P388 cell line (46,47)
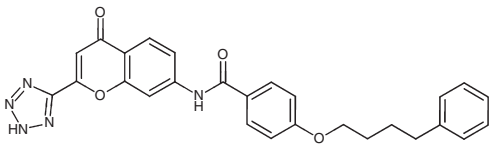	481.55	4.673	2	8	Pranlukast Antiasthmatic Leukotriene antagonist	No data

Table 1: (*Continued*)

Structure	Molecular weight	ALogP	Hydrogen bond donors	Hydrogen bond acceptors	Name/activity (http://pubchem.ncbi.nlm.nih.gov/)	Described ATP-binding cassette transporters modulation
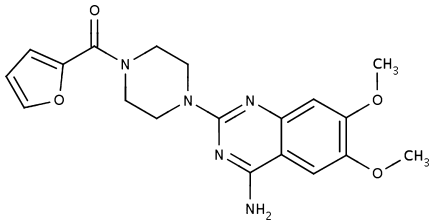	383.45	2.108	2	9	Prazosin Selective adrenergic α-1 antagonist Used in the treatment of heart failure and hypertension, pheochromocytoma, Raynaud's syndrome, prostatic hypertrophy, and urinary retention	P-gp substrate, stimulating P-gp-mediated transport. It was hypothesized to bind to a third drug-binding site on P-gp, an allosteric site that is likely not capable of drug transport (48)
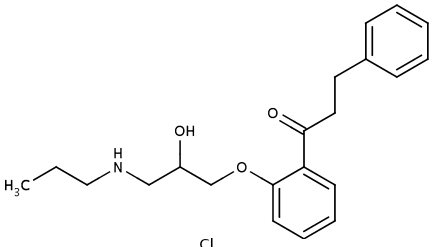	341.49	3.673	2	4	Propafenone Antiarrhythmic agent Weak β-blocking activity	Potent inhibitor of P-gp-mediated efflux, stimulating ATPase activity (49)
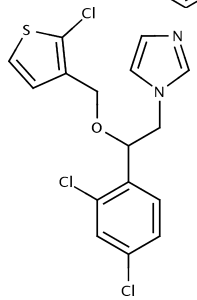	387.73	4.438	0	2	Tioconazole Antifungal agent	Itraconazole and Ketoconazole inhibit P-gp function (43); there is no reference to Tioconazole
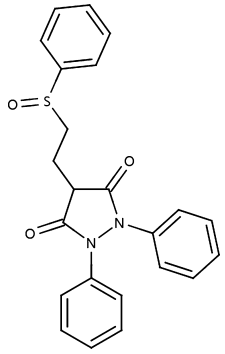	404.52	3.434	0	5	Sulfinpyrazone Uricosuric agent	Described as MRP modulator (50)

Table 1: (*Continued*)

Structure	Molecular weight	ALogP	Hydrogen bond donors	Hydrogen bond acceptors	Name/activity (http://pubchem.ncbi.nlm.nih.gov/)	Described ATP-binding cassette transporters modulation
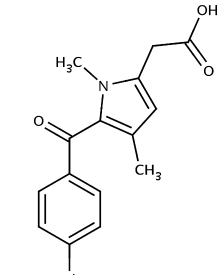	291.75	3.906	1	3	Zomepirac NSAID with antipyretic activity	Enhances the cytotoxicity of certain anticancer drugs in MRP-overexpressing cell lines suggesting possible MRP-modulation profile (51)
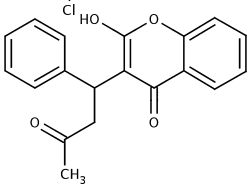	308.35	3.128	1	4	Warfarin Anticoagulant Inhibitor of the synthesis of vitamin K-dependent coagulation factors	Preliminary evidence that P-gp contributes to Warfarin disposition (52)

ALogP, atom-based module for logP; MRP, multidrug-resistance protein.

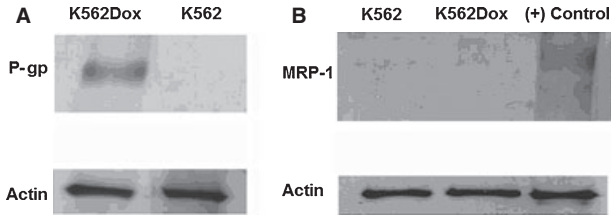

Figure 3: Expression of P-gp and MRP-1 proteins on K562 and K562Dox cell lines. Proteins were extracted and analyzed by Western blot. Actin was used as a loading control. Representative results of at least three independent experiments are shown. (A) P-gp expression is detected in the K562Dox but not in the K562 cell line; (B) No MRP-1 expression is detected in either K562 or K562Dox cell lines, but is present in the positive control.

elucidate if the drugs that caused accumulation of rh123 were either substrates for transport by P-gp (competitive ligands), or P-gp inhibitors (non-competitive ligands), effects on the ATPase activity of P-gp were measured using human P-gp membranes (65). The results for twelve drugs are presented in Figure 5. The assay relies on the ATP dependence of the light-generating reaction of firefly luciferase. ATP is first incubated with P-gp, then the P-gp ATPase reaction is stopped, and the remaining ATP is detected as a luciferase-generated luminescent signal. P-gp-dependent decreases in luminescence reflect ATP consumption by P-gp; thus, the greater the decrease in signal the higher the P-gp activity. Accordingly, samples containing compounds that stimulate the P-gp ATPase will have significantly lower signals than untreated samples[a]. Five controls were used: no treatment (NT) control, sodium orthovanadate (Na_3VO_4), verapamil, mibefradil and quinidine treatments. Na_3VO_4 is an inhibitor of the P-gp ATPase (66), so this compound serves as a control where residual P-gp-dependent ATP-consumption occurs. Therefore, this control causes an increase in the % of luminescence of luciferase in relation to the untreated (NT) control (Figure 5, left). On the other hand, verapamil, mibefradil and quinidine are substrates for transport by P-gp that stimulate P-gp ATPase activity. As shown in Figure 5, these controls cause a significantly decrease in the % of luminescence of luciferase in relation to the untreated (NT) control.

Econazole, amoxapine, loxapine, bicalutamide, zomepirac, and tioconazole caused an increase in the % of luminescence in relation to the untreated (NT) control showing an effect compatible with P-gp ATPase inhibition. From these inhibitors, six were found to prevent ATP hydrolysis (Figure 5), blocking P-gp catalytic cycle without being transported, thus possibly targeting the P-gp's ATP binding site directly (67,68) or by binding to an allosteric residue (69,70) which causes inhibition of P-gp function with resulting inhibition of ATPase activity. As could be expected, econazole, similarly to other antifungal compounds from the azole family previously described as P-gp inhibitors, also causes P-gp inhibition by a non-competitive mechanism. It gives origin to a % luminescence in the ATPase assay similar to that of the control Na_3VO_4 and therefore it could also be used as a control in this type of assays. Interestingly, econazole had already been described as inhibitor of other ATPases such as Ca^{2+}-ATPase (71). Further understanding of the potential location of the site of action of these molecules would require a systematic analysis of the ATPase profile of combinations of verapamil and other transporter substrates with the new P-gp modulators (63,64), or even more thoroughly, cystein scanning mutagenesis (72,73). On the other hand, loxapine and amoxapine, known tricyclic antidepressants, were found to be potent non-competitive P-gp inhibitors. These compounds share a common scaffold for the development of new P-gp inhibitors. Propafenone, hycanthone, cyclic pifithryn-α, diltiazem, azelastine, and prazosin behave similarly to verapamil,

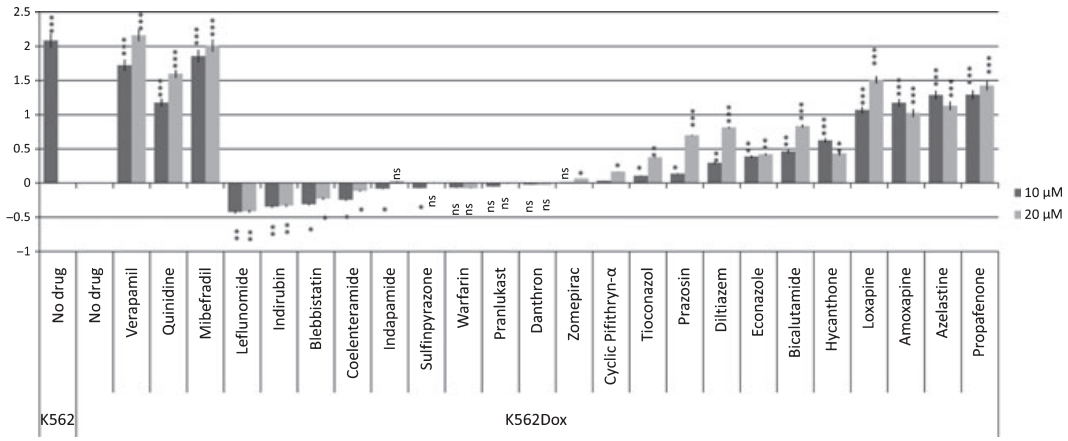

Figure 4: Accumulation ratios of rh123 after 1 h of incubation in K562 or K562Dox cell lines. Results are the average of three independent experiments ± SE. Statistical significance was tested by paired *t*-test using the untreated K562Dox (second entry) as control. *** indicates $p < 0.001$; ** indicates $0.001 < p \leq 0.01$; * indicates $0.01 < p \leq 0.05$. ns indicate not significant, i.e., $p > 0.05$ ($n = 3$).

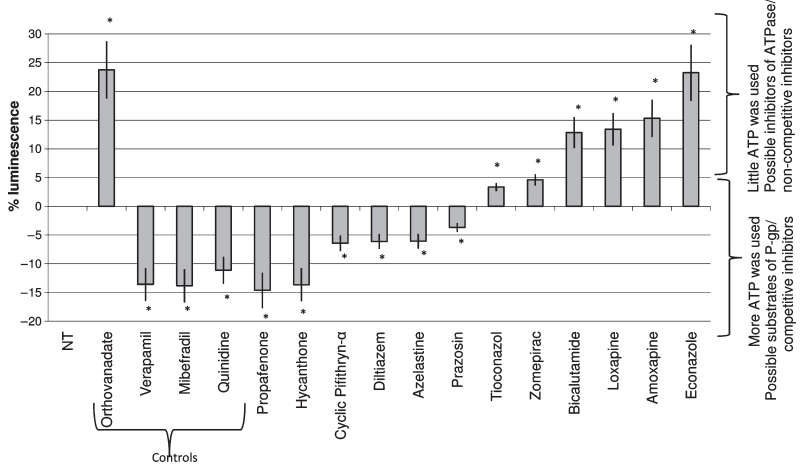

Figure 5: P-gp ATPase assay. Results are % of relative light unit (RLU) in relation to non-treated (NT) control. NT control luminescence is represented as zero for easier interpretation. % of RLU superior to zero corresponds to inhibitors of P-gp ATPase, i.e., non-competitive P-gp inhibitors. % of RLU inferior to zero correspond to substrates of P-gp, i.e., competitive P-gp inhibitors. Results are the mean ± SE of three independent experiments. Na_3VO_4, verapamil, mibefradil, and quinidine were used as controls. Statistical significance was tested by paired *t*-test using the NT control as a negative control. * indicates $0.01 < p \leq 0.05$ ($n = 3$).

mibefradil, and quinidine, i.e., they increased the hydrolysis of ATP by P-gp, indicating that they are competitive inhibitors of P-gp, possibly being themselves transported by the pump. Thus, it is possible to conclude that from the twelve compounds that had caused accumulation of rh123 in the cells, half are acting as competitive and the other half as non-competitive inhibitors of P-gp.

Most of the compounds already described in the literature as interacting with P-gp were found to have the same kind of modulatory behavior as previously described, which reinforces our findings. However, cyclic pifithryn-α is described elsewhere (41) as an activator and our experiments revealed it as an inhibitor (both substrates of P-gp). Differences in cell models (human ovarian cancer cell lines A2780 and A2780 Adr), accumulation assay (1 and 10 µM; 2-h incubation) and ATPase assay conditions (1 and 3 µM) may justify this difference. On the other hand, our experiments revealed bicalutamide as a non-competitive inhibitor while it was previously described (40) as a P-gp substrate. Also, different assays (1–100 µM, Caco-2 and calcein-AM assays) may be the cause of the divergent results.

Correlations between the ATPase assay (Figure 5) and the rh123 accumulation assay (Figure 4) could be observed for some of the investigated compounds. Most of the compounds with the highest inhibitory ratio (>1) in the rh123 accumulation assay, such as propafenone, amoxapine, and loxapine, also showed a high effect in the ATPase assay. Nevertheless, azelastine, with an accumulation ratio of rh123 > 1, did not show the same relative potency in

the ATPase assay. The opposite can be observed for econazole, which presented the highest relative % of luminescence in the ATPase assay but an accumulation ratio of rh123 < 0.5. This discrepancy in the relative potency of some of the drugs is probably due to the fact that the rh123 accumulation assay uses cells and the ATPase assay uses membrane fractions. In this assay, a substantial portion of the recombinant P-gp membranes are open fragments and 'inside-out' vesicles, and therefore, it is not so influenced by factors related to drug permeability (74,75). Other possible justification for the discrepancies found between the two assays is the possible different mechanisms/binding sites involved in the P-gp modulation, making it difficult to establish relationships between the two assays.

Cell growth assay

To better understand the potential of the newly found P-gp inhibitors, their effect in the cytotoxicity of doxorubicin in the cell line overexpressing P-gp (K562Dox) was investigated. Results of the SRB assay are presented in Table 2 for the nine most active inhibitors (Figure 1IV).

The drugs were firstly tested individually in the K562Dox cell line to verify if they were cytotoxic themselves, which would cause an increase in the cytotoxicity of doxorubicin but not because of P-gp modulation. Only the control, doxorubicin itself, showed a cytotoxic effect (GI_{50} = 11.62 ± 1.14 μM) in this resistant cell line (Table 2A). When testing doxorubicin in combination with 10 μM of the test drug, all drugs were able to decrease the value of doxorubicin GI_{50} (Table 2B). As expected, verapamil (76) and quinidine (77) (positive controls) also decreased the GI_{50} of doxorubicin; this decrease was approximately 6-fold (Table 2B). The nine investigated drugs were found to inhibit P-gp activity in the K562Dox cell line, being able to decrease the GI_{50} of doxorubicin from 11.62 μM up to 3.16 μM (Table 2). From the investigated compounds, econazole showed the most potent effect, decreasing 3.7 times the GI_{50} of doxorubicin. Amoxapine and loxapine caused a 3.5-fold decrease in the GI_{50} of doxorubicin, and for prazosin and bicalutamide, a 3.1 and 3.0-fold decrease was observed, respectively. In fact, all the investigated drugs decreased the GI_{50} of doxorubicin in a statistically significant manner, except for propafenone and diltiazem and the control mibefradil. Thus, we may hypothesize that the long-term (48 h) incubation of a P-gp overexpressing cell line with a cytotoxic agent (doxorubicin) in combination with these drugs decreased the GI_{50} of the cytotoxic agent by reducing the activity of P-gp.

Table 2: Results from the sulphorhodamine-B assay in K562Dox cells. (A) GI_{50} values calculated for test drugs and doxorubicin, (B) GI_{50} values of doxorubicin in combination with 10 μM of the test drugs and (C) correspondent GI_{50} decrease ratio

	GI_{50} (μM) in K562Dox cells		(C) Decrease ratio in the GI_{50} of doxorubicin
	(A) GI_{50} of test compounds	(B) GI_{50} of doxorubicin with 10 μM of test compounds	
Controls			
Verapamil	>150	1.96 ± 0.03***	5.9
Quinidine	>150	1.98 ± 0.07***	5.9
Mibefradil	>150	8.49 ± 1.23ns	1.4
Econazole	>150	3.16 ± 0.41**	3.7
Loxapine	>150	3.35 ± 0.66**	3.5
Amoxapine	>150	3.28 ± 0.7**	3.5
Prazosin	>150	3.74 ± 0.61**	3.1
Bicalutamide	>150	3.90 ± 0.5**	3.0
Azelastine	>150	6.49 ± 0.29*	1.8
Hycanthone	>150	8.45 ± 0.6*	1.4
Propafenone	>150	9.82 ± 1.52ns	1.2
Diltiazem	>150	10.27 ± 1.27ns	1.1
Doxorubicin	11.62 ± 1.14		

The results are presented as mean ± SE of at least three independent experiments. Statistical significance was tested by paired *t*-test using the GI_{50} doxorubicin alone in K562Dox cell line as control. ns indicates non-significant (n = 3).
*0.01 < p ≤ 0.05; **0.001 < p ≤ 0.01; ***p ≤ 0.001.

Principal component analysis

In order to visualize structural diversity/similarity between these different classes of drugs, a PCA was performed (Figure 1V). Plotting the principal components is a method to visualize the maximum variability of the data points. A PCA based on the properties of the 24 molecules was performed. The PCA was projected onto the 3D principal components plane (Figure 6). It provides a 3D representation of the closeness of the structural relationships between the samples.

The first component PC1 (which explains 46.0% of the variance in the biologic response), the second component PC2 (33.7%), and the third component PC3 (9.2%) account for 88.9% of the total variance in the data. Figure 6 shows two small clusters corresponding to different classes of molecules. It clearly demonstrates segregation between blue (inhibitors) and yellow (activators) circles (Figure 6).

Inspection of Table 3 shows that the principal components result mainly from the linear combination of descriptors related to the effect of hydrophilicity/lipophilicity and number of hydrogen-bond donors and acceptors. This is consistent with the well known and described importance of a certain degree of hydrophobicity (78,79) and presence of groups that act as hydrogen-bond donors and/or acceptors, such as amines (78–80), in molecules that interact with P-gp, and also consistent with several published structure–activity studies for P-gp modulation (81–83) which identified structural features reflecting the presence of amphiphilic nature groups and hydrogen bond acceptor in compounds that interact with P-gp.

Conclusion

A pharmacophore model was developed for the screening of potential P-gp inhibitors in the DrugBank database. The successful identification among the retrieved hits of novel P-gp inhibitors and the demonstration of their activities indicated that this is a valuable approach to discover novel non-label uses for known drugs. Potent inhibitors with a dibenzoxazepine scaffold emerged from this study

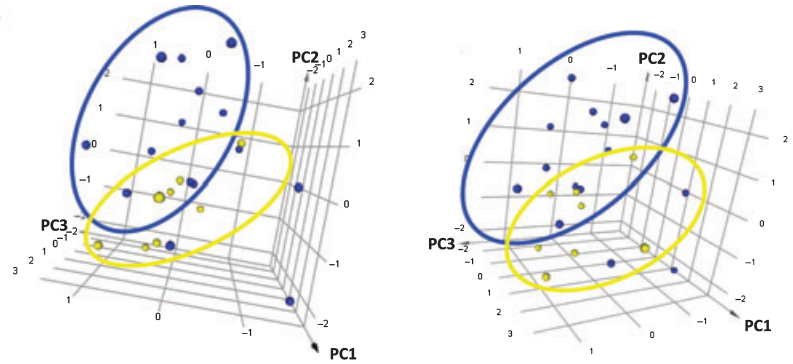

Component	Variance explained (%)	Cumulative variance explained (%)
PC1	46.0	46.0
PC2	33.7	79.7
PC3	9.2	88.9

Figure 6: (A) Front view and (B) top view of principal component analysis of the 24 tested compounds. Yellow: activators; Blue: inhibitors (both competitive and non-competitive). (C) Explained variance of principal components.

Table 3: Loadings of principal component analysis

Descriptors	PC1	PC2	PC3
Constant	−6.9282	−1.5179	0.1023
ALogP	0.2060	0.6017	0.3760
Molecular weight	0.0079	0.0034	−0.0035
Number of hydrogen bond donors	0.2305	−0.5794	0.8698
Number of hydrogen bond acceptors	0.3096	−0.1719	−0.2400
Number of rotatable bonds	0.1417	0.0912	0.0694
Molecular polar surface area	0.0168	−0.0155	−0.0055

ALogP, atom-based module for logP.

and they will be further investigated in order to develop new more effective and safe P-gp inhibitors.

Acknowledgments

FCT (I&D, no. 226/2003 and I&D, no. 4040/07), FEDER, POCI, U.Porto and Santander Totta for financial support. IPATIMUP is an Associate Laboratory of the Portuguese Ministry of Ministry of Science, Technology and Higher Education and is partially supported by FCT, the Portuguese Foundation for Science and Technology.

References

1. Higgins C.F. (2007) Multiple molecular mechanisms for multidrug resistance transporters. Nature;446:749–757.
2. Kaszubiak A., Kupstat A., Muller U., Hausmann R., Holm P.S., Lage H. (2007) Regulation of MDR1 gene expression in multidrug-resistant cancer cells is independent from YB-1. Biochem Biophys Res Commun;357:295–301.
3. Vecchio S.D., Ciarmiello A., Potena M.I., Carriero M.V., Mainolfi C., Botti G., Thomas R., Cerra M., D'aiuto G., Tsuruo T., Salvatore M. (1997) *In vivo* detection of multidrug-resistant (MDR1) phenotype by technetium-99m sestamibi scan in untreated breast cancer patients. Eur J Nucl Med;24:150–159.
4. Kaur P. (2002) Multidrug resistance: can different keys open the same lock? Drug Resist Updat;5:61–64.
5. Higgins C.F. (1993) The multidrug resistance P-glycoprotein. Curr Opin Cell Biol;5:684–687.
6. Clarke R., Leonessa F., Trock B. (2005) Multidrug resistance/P-glycoprotein and breast cancer: review and meta-analysis. Semin Oncol;32:S9–S15.
7. Teodori E., Dei S., Scapecchi S., Gualtieri F. (2002) The medicinal chemistry of multidrug resistance (MDR) reversing drugs. Farmaco;57:385–415.
8. Higgins C.F., Callaghan R., Linton K.J., Rosenberg M.F., Ford R.C. (1997) Structure of the multidrug resistance P-glycoprotein. Semin Cancer Biol;8:135–142.
9. Johnstone R.W., Ruefli A.A., Smyth M.J. (2000) Multiple physiological functions for multidrug transporter P-glycoprotein? Trends Biochem Sci;25:1–6.
10. Badhan R., Penny J., Galetin A., Houston J.B. (2009) Methodology for development of a physiological model incorporating CYP3A and P-glycoprotein for the prediction of intestinal drug absorption. J Pharm Sci;98:2180–2197.
11. Hassan H.E., Myers A.L., Coop A., Eddington N.D. (2009) Differential involvement of P-glycoprotein (ABCB1) in permeability, tissue distribution, and antinociceptive activity of methadone, buprenorphine, and diprenorphine: *in vitro* and *in vivo* evaluation. J Pharm Sci;98:4928–4940.
12. Zhou S.F., Xue C.C., Yu X.Q., Li C., Wang G. (2007) Clinically important drug interactions potentially involving mechanism-based inhibition of cytochrome P450 3A4 and the role of therapeutic drug monitoring. Ther Drug Monit;29:687–710.
13. Benet L.Z. (2009) The drug transporter-metabolism alliance: uncovering and defining the interplay. Mol Pharm;6:1631–1643.

14. Zhou S.F. (2008) Drugs behave as substrates, inhibitors and inducers of human cytochrome P450 3A4. Curr Drug Metab;9:310–322.
15. Szakacs G., Varadi A., Ozvegy-Laczka C., Sarkadi B. (2008) The role of ABC transporters in drug absorption, distribution, metabolism, excretion and toxicity (ADME-Tox). Drug Discov Today;13:379–393.
16. Thiel-Demby V.E., Tippin T.K., Humphreys J.E., Serabjit-Singh C.J., Polli J.W. (2004) *In vitro* absorption and secretory quotients: practical criteria derived from a study of 331 compounds to assess for the impact of P-glycoprotein-mediated efflux on drug candidates. J Pharm Sci;93:2567–2572.
17. Campillos M., Kuhn M., Gavin A.C., Jensen L.J., Bork P. (2008) Drug target identification using side-effect similarity. Science;321:263–266.
18. Pal D., Mitra A.K. (2006) MDR- and CYP3A4-mediated drug-drug interactions. J Neuroimmune Pharmacol;1:323–339.
19. Huang S.M., Woodcock J. (2010) Transporters in drug development: advancing on the Critical Path. Nat Rev Drug Discov;9:175–176.
20. Polli J.W., Baughman T.M., Humphreys J.E., Jordan K.H., Mote A.L., Salisbury J.A., Tippin T.K., Serabjit-Singh C.J. (2003) P-glycoprotein influences the brain concentrations of cetirizine (Zyrtec), a second-generation non-sedating antihistamine. J Pharm Sci;92:2082–2089.
21. Loo T.W., Clarke D.M. (1999) Determining the structure and mechanism of the human multidrug resistance P-glycoprotein using cysteine-scanning mutagenesis and thiol-modification techniques. Biochim Biophys Acta;1461:315–325.
22. Rosenberg M.F., Callaghan R., Modok S., Higgins C.F., Ford R.C. (2005) Three-dimensional structure of P-glycoprotein: the transmembrane regions adopt an asymmetric configuration in the nucleotide-bound state. J Biol Chem;280:2857–2862.
23. Cianchetta G., Singleton R.W., Zhang M., Wildgoose M., Giesing D., Fravolini A., Cruciani G., Vaz R.J. (2005) A pharmacophore hypothesis for P-glycoprotein substrate recognition using GRIND-based 3D-QSAR. J Med Chem;48:2927–2935.
24. Li W.X., Li L., Eksterowicz J., Ling X.B., Cardozo M. (2007) Significance analysis and multiple pharmacophore models for differentiating P-glycoprotein substrates. J Chem Inf Model;47:2429–2438.
25. Pajeva I.K., Wiese M. (2002) Pharmacophore model of drugs involved in P-glycoprotein multidrug resistance: explanation of structural variety (hypothesis). J Med Chem;45:5671–5686.
26. Penzotti J.E., Lamb M.L., Evensen E., Grootenhuis P.D. (2002) A computational ensemble pharmacophore model for identifying substrates of P-glycoprotein. J Med Chem;45:1737–1740.
27. Boccard J., Bajot F., Di Pietro A., Rudaz S., Boumendjel A., Nicolle E., Carrupt P.A. (2009) A 3D linear solvation energy model to quantify the affinity of flavonoid derivatives toward P-glycoprotein. Eur J Pharm Sci;36:254–264.
28. Boumendjel A., Di Pietro A., Dumontet C., Barron D. (2002) Recent advances in the discovery of flavonoids and analogs with high-affinity binding to P-glycoprotein responsible for cancer cell multidrug resistance. Med Res Rev;22:512–529.
29. Froimowitz M. (1993) HyperChem: a software package for computational chemistry and molecular modeling. BioTechniques;14:1010–1013.
30. Grippo L., Lucidi S. (1997) A globally convergent version of the Polak-Ribière conjugate gradient method. Math Program;78:375–391.
31. Schneidman-Duhovny D., Dror O., Inbar Y., Nussinov R., Wolfson H.J. (2008) PharmaGist: a webserver for ligand-based pharmacophore detection. Nucleic Acids Res;36:W223–W228.
32. Wishart D.S., Knox C., Guo A.C., Cheng D., Shrivastava S., Tzur D., Gautam B., Hassanali M. (2008) DrugBank: a knowledgebase for drugs, drug actions and drug targets. Nucleic Acids Res;36:D901–D906.
33. Lima R.T., Martins L.M., Guimaraes J.E., Sambade C., Vasconcelos M.H. (2004) Specific downregulation of bcl-2 and xIAP by RNAi enhances the effects of chemotherapeutic agents in MCF-7 human breast cancer cells. Cancer Gene Ther;11:309–316.
34. Houghton P., Fang R., Techatanawat I., Steventon G., Hylands P.J., Lee C.C. (2007) The sulphorhodamine (SRB) assay and other approaches to testing plant extracts and derived compounds for activities related to reputed anticancer activity. Methods;42:377–387.
35. Chong C.R., Sullivan D.J. Jr (2007) New uses for old drugs. Nature;448:645–646.
36. Wermuth C.G. (2004) Selective optimization of side activities: another way for drug discovery. J Med Chem;47:1303–1314.
37. Wermuth C.G. (2006) Selective optimization of side activities: the SOSA approach. Drug Discov Today;11:160–164.
38. Lipinski C.A. (2003) Chris Lipinski discusses life and chemistry after the Rule of Five. Drug Discov Today;8:12–16.
39. Yan Ping H., Robert J. (1995) Azelastine and flezelastine as reversing agents of multidrug resistance: pharmacological and molecular studies. Biochem Pharmacol;50:169–175.
40. Colabufo N.A., Pagliarulo V., Berardi F., Contino M., Inglese C., Niso M., Ancona P., Albo G., Perrone R. (2008) Bicalutamide failure in prostate cancer treatment: involvement of Multi Drug Resistance proteins. Eur J Pharmacol;601:38–42.
41. Sterz K., Mollmann L., Jacobs A., Baumert D., Wiese M. (2009) Activators of P-glycoprotein: structure-activity relationships and investigation of their mode of action. ChemMedChem;4:1897–1911.
42. Molden E., Christensen H., Sund R.B. (2000) Extensive metabolism of diltiazem and P-glycoprotein-mediated efflux of desacetyl-diltiazem (M1) by rat jejunum *in vitro*. Drug Metab Dispos;28:107–109.
43. Wang E.J., Lew K., Casciano C.N., Clement R.P., Johnson W.W. (2002) Interaction of common azole antifungals with P glycoprotein. Antimicrob Agents Chemother;46:160–165.
44. Efferth T., Volm M. (1993) Reversal of doxorubicin-resistance in sarcoma 180 tumor cells by inhibition of different resistance mechanisms. Cancer Lett;70:197–202.
45. Kis E., Nagy T., Jani M., Molnar E., Janossy J., Ujhellyi O., Német K., Herédi-Szabó K., Krajcsi P. (2009) Leflunomide and its metabolite A771726 are high affinity substrates of BCRP: implications for drug resistance. Ann Rheum Dis;68:1201–1207.
46. Ramu A., Ramu N. (1992) Reversal of multidrug resistance by phenothiazines and structurally related compounds. Cancer Chemother Pharmacol;30:165–173.
47. Zsila F. (2007) Overlapping ligand specificity of P-glycoprotein and serum alpha(1)-acid glycoprotein: evidences and potential implications. Curr Drug Metab;8:563–593.
48. Shapiro A.B., Fox K., Lam P., Ling V. (1999) Stimulation of P-glycoprotein-mediated drug transport by prazosin and progesterone. Evidence for a third drug-binding site. Eur J Biochem;259:841–850.

49. Schmid D., Ecker G., Kopp S., Hitzler M., Chiba P. (1999) Structure-activity relationship studies of propafenone analogs based on P-glycoprotein ATPase activity measurements. Biochem Pharmacol;58:1447–1456.
50. Hollo Z., Homolya L., Hegedus T., Sarkadi B. (1996) Transport properties of the multidrug resistance-associated protein (MRP) in human tumour cells. FEBS Lett;383:99–104.
51. Duffy C.P., Elliott C.J., O'Connor R.A., Heenan M.M., Coyle S., Cleary I.M., Kavanagh K., Verhaegen S., O'Loughlin C.M., NicAmhlaoibh R., Clunes M. (1998) Enhancement of chemotherapeutic drug toxicity to human tumour cells *in vitro* by a subset of non-steroidal anti-inflammatory drugs (NSAIDs). Eur J Cancer;34:1250–1259.
52. Sussman N. (2002) The predictive nature of high throughput toxicity screening using a human hepatocyte cell line. Cell Notes;3:7–10.
53. Kim R.B. (2002) Drugs as P-glycoprotein substrates, inhibitors, and inducers. Drug Metab Rev;34:47–54.
54. Wandel C., Kim R.B., Guengerich F.P., Wood A.J. (2000) Mibefradil is a P-glycoprotein substrate and a potent inhibitor of both P-glycoprotein and CYP3A *in vitro*. Drug Metab Dispos;28:895–898.
55. Tatu C.A., Paunescu V., Stanescu D.I., Schneider F. (1997) P-glycoprotein mediated multidrug resistance assessment by flow-cytometry in malignant hemopathies. Anticancer Res;17:2583–2586.
56. Wang E.J., Casciano C.N., Clement R.P., Johnson W.W. (2000) *In vitro* flow cytometry method to quantitatively assess inhibitors of P-glycoprotein. Drug Metab Dispos;28:522–528.
57. Akazawa Y., Kawaguchi H., Funahashi M., Watanabe Y., Yamaoka K., Hashida M., Takakura Y. (2002) Effect of interferons on P-glycoprotein-mediated rhodamine-123 efflux in cultured rat hepatocytes. J Pharm Sci;91:2110–2115.
58. Ludescher C., Thaler J., Drach D., Drach J., Spitaler M., Gattringer C., Huber H., Hofmann J. (1992) Detection of activity of P-glycoprotein in human tumour samples using rhodamine 123. Br J Haematol;82:161–168.
59. Petriz J., Garcia-Lopez J. (1997) Flow cytometric analysis of P-glycoprotein function using rhodamine 123. Leukemia;11:1124–1130.
60. Efferth T., Dunn T.A., Berlion M., Langenbahn H., Pommerenke E.W., Volm M. (1993) Reversal of inherent multidrug-resistance in primary human renal cell carcinoma cell cultures by S 9788. Anticancer Res;13:905–908.
61. Denis-Gay M., Petit J.M., Ratinaud M.H. (1995) Rhodamine 123: is it an appropriate dye to study P-glycoprotein activity in adriamycin-resistant K562 cells? Anticancer Res;15:121–126.
62. Slapak C.A., Mizunuma N., Kufe D.W. (1994) Expression of the multidrug resistance associated protein and P-glycoprotein in doxorubicin-selected human myeloid leukemia cells. Blood;84:3113–3121.
63. Garrigos M., Mir L.M., Orlowski S. (1997) Competitive and non-competitive inhibition of the multidrug-resistance-associated P-glycoprotein ATPase–further experimental evidence for a multisite model. Eur J Biochem;244:664–673.
64. Litman T., Zeuthen T., Skovsgaard T., Stein W.D. (1997) Competitive, non-competitive and cooperative interactions between substrates of P-glycoprotein as measured by its ATPase activity. Biochim Biophys Acta;1361:169–176.
65. Belli S., Elsener P.M., Wunderli-Allenspach H., Kramer S.D. (2009) Cholesterol-mediated activation of P-glycoprotein: distinct effects on basal and drug-induced ATPase activities. J Pharm Sci;98:1905–1918.
66. Urbatsch I.L., al-Shawi M.K., Senior A.E. (1994) Characterization of the ATPase activity of purified Chinese hamster P-glycoprotein. Biochemistry;33:7069–7076.
67. Tchamo D.N., Dijoux-Franca M.G., Mariotte A.M., Tsamo E., Daskiewicz J.B., Bayet C., Barron D., Conseil G., Pietro A. (2000) Prenylated xanthones as potential P-glycoprotein modulators. Bioorg Med Chem Lett;10:1343–1345.
68. Dayan G., Jault J.M., Baubichon-Cortay H., Baggetto L.G., Renoir J.M., Baulieu E.E., Gros P., Di Pietro A. (1997) Binding of steroid modulators to recombinant cytosolic domain from mouse P-glycoprotein in close proximity to the ATP site. Biochemistry;36:15208–15215.
69. Maki N., Hafkemeyer P., Dey S. (2003) Allosteric modulation of human P-glycoprotein. Inhibition of transport by preventing substrate translocation and dissociation. J Biol Chem;278:18132–18139.
70. Martin C., Berridge G., Higgins C.F., Callaghan R. (1997) The multi-drug resistance reversal agent SR33557 and modulation of vinca alkaloid binding to P-glycoprotein by an allosteric interaction. Br J Pharmacol;122:765–771.
71. Mason M.J., Mayer B., Hymel L.J. (1993) Inhibition of Ca^{2+} transport pathways in thymic lymphocytes by econazole, miconazole, and SKF 96365. Am J Physiol;264:C654–C662.
72. Loo T.W., Clarke D.M. (1999) Identification of residues in the drug-binding domain of human P-glycoprotein. Analysis of transmembrane segment 11 by cysteine-scanning mutagenesis and inhibition by dibromobimane. J Biol Chem;274:35388–35392.
73. Loo T.W., Clarke D.M. (2000) Identification of residues within the drug-binding domain of the human multidrug resistance P-glycoprotein by cysteine-scanning mutagenesis and reaction with dibromobimane. J Biol Chem;275:39272–39278.
74. Eytan G.D., Regev R., Assaraf Y.G. (1996) Functional reconstitution of P-glycoprotein reveals an apparent near stoichiometric drug transport to ATP hydrolysis. J Biol Chem;271:3172–3178.
75. Dongping M. (2007) Identify P-glycoprotein Substrates and Inhibitors with the Rapid, HTS Pgp-Glo™ Assay System. Promega Notes;96:11–14.
76. Shoji Y., Fisher M.H., Periasamy A., Herman B., Juliano R.L. (1991) Verapamil and cyclosporin A modulate doxorubicin toxicity by distinct mechanisms. Cancer Lett;57:209–218.
77. Vezmar M., Georges E. (2000) Reversal of MRP-mediated doxorubicin resistance with quinoline-based drugs. Biochem Pharmacol;59:1245–1252.
78. Chiba P., Ecker G., Schmid D., Drach J., Tell B., Goldenberg S., Gekeler V. (1996) Structural requirements for activity of propafenone-type modulators in P-glycoprotein-mediated multidrug resistance. Mol Pharmacol;49:1122–1130.
79. Zamora J.M., Pearce H.L., Beck W.T. (1988) Physical-chemical properties shared by compounds that modulate multidrug resistance in human leukemic cells. Mol Pharmacol;33:454–462.
80. Ecker G., Huber M., Schmid D., Chiba P. (1999) The importance of a nitrogen atom in modulators of multidrug resistance. Mol Pharmacol;56:791–796.
81. Muller H., Pajeva I.K., Globisch C., Wiese M. (2008) Functional assay and structure-activity relationships of new third-

generation P-glycoprotein inhibitors. Bioorg Med Chem;16: 2448–2462.
82. Reyes C.P., Munoz-Martinez F., Torrecillas I.R., Mendoza C.R., Gamarro F., Bazzocchi I.L., Núñez M.J., Pardo L., Castanys S., Campillo M., Jiménez I.A. (2007) Biological evaluation, structure-activity relationships, and three-dimensional quantitative structure-activity relationship studies of dihydro-beta-agarofuran sesquiterpenes as modulators of P-glycoprotein-dependent multidrug resistance. J Med Chem;50:4808–4817.
83. Gombar V.K., Polli J.W., Humphreys J.E., Wring S.A., Serabjit-Singh C.S. (2004) Predicting P-glycoprotein substrates by a quantitative structure-activity relationship model. J Pharm Sci;93:957–968.

Note

[a]Promega. Technical Bulletin – Pgp-Glo^{TM} Assay Systems In: http://www.promega.com/tbs/tb341/tb341.pdf, editor. Technical Bulletin – Pgp-Glo^{TM} Assay Systems.

Supporting Information

Additional Supporting Information may be found in the online version of this article:

Appendix S1. Flavone (A), dehydrosylibin (B) and chalcone (C) derivates used to build pharmacophore models for the P-gp target.

Please note: Wiley-Blackwell is not responsible for the content or functionality of any supporting materials supplied by the authors. Any queries (other than missing material) should be directed to the corresponding author for the article.